4-1-2021

Responses of stomatal features and photosynthesis to porewater N enrichment and elevated atmospheric CO2 in Phragmites australis, the common reed

Julian R. Garrison
Bowdoin College

Joshua S. Caplan
Temple University

Vladimir Douhovnikoff
Bowdoin College

Thomas J. Mozdzer
Bryn Mawr College

Barry A. Logan
Bowdoin College

BRIEF COMMUNICATIONS

American Journal of Botany

BRIEF COMMUNICATION

Responses of stomatal features and photosynthesis to porewater N enrichment and elevated atmospheric CO_2 in *Phragmites australis*, the common reed

Julian R. Garrison[1], Joshua S. Caplan[2], Vladimir Douhovnikoff[1], Thomas J. Mozdzer[3], and Barry A. Logan[1,4]

Manuscript received 20 February 2020; revision accepted 15 December 2020.

[1] Biology Department, Bowdoin College, Brunswick, ME 04011, USA

[2] Department of Architecture & Environmental Design, Temple University, Ambler, PA 19002, USA

[3] Biology Department, Bryn Mawr College, Bryn Mawr, PA 19010, USA

[4] Author for correspondence (e-mail: blogan@bowdoin.edu)

Citation: Garrison, J. R., J. S. Caplan, V. Douhovnikoff, T. J. Mozdzer, and B. A. Logan. 2021. Responses of stomatal features and photosynthesis to porewater N enrichment and elevated atmospheric CO_2 in *Phragmites australis*, the common reed. *American Journal of Botany* 108(4): 718–725.

doi:10.1002/ajb2.1638

PREMISE: Biological invasions increasingly threaten native biodiversity and ecosystem services. One notable example is the common reed, *Phragmites australis*, which aggressively invades North American salt marshes. Elevated atmospheric CO_2 and nitrogen pollution enhance its growth and facilitate invasion because *P. australis* responds more strongly to these enrichments than do native species. We investigated how modifications to stomatal features contribute to strong photosynthetic responses to CO_2 and nitrogen enrichment in *P. australis* by evaluating stomatal shifts under experimental conditions and relating them to maximal stomatal conductance (g_{wmax}) and photosynthetic rates.

METHODS: Plants were grown *in situ* in open-top chambers under ambient and elevated atmospheric CO_2 (eCO_2) and porewater nitrogen (N_{enr}) in a Chesapeake Bay tidal marsh. We measured light-saturated carbon assimilation rates (A_{sat}) and stomatal characteristics, from which we calculated g_{wmax} and determined whether CO_2 and N_{enr} altered the relationship between g_{wmax} and A_{sat}.

RESULTS: eCO_2 and N_{enr} enhanced both g_{wmax} and A_{sat}, but to differing degrees; g_{wmax} was more strongly influenced by N_{enr} through increases in stomatal density while A_{sat} was more strongly stimulated by eCO_2. There was a positive relationship between g_{wmax} and A_{sat} that was not modified by eCO_2 or N_{enr}, individually or in combination.

CONCLUSIONS: Changes in stomatal features co-occur with previously described responses of *P. australis* to eCO_2 and N_{enr}. Complementary responses of stomatal length and density to these global change factors may facilitate greater stomatal conductance and carbon gain, contributing to the invasiveness of the introduced lineage.

KEY WORDS carbon dioxide; environmental scanning electron microscopy (ESEM); guard cell length; leaf surface features; nitrogen eutrophication; Poaceae.

Owing to the accelerating pace of globalization, biological invasions increasingly threaten native biodiversity and ecosystem functions (Groom, 2006; Katsanevakis et al., 2014; Vila and Hulme, 2017). One of the world's most prolific invaders is the common reed, *Phragmites australis* (Cav.) Trin. ex Steud., a well-described species and promising model organism for studying invasive plants and their responses to global change (Eller et al., 2017; Cesarino et al., 2020). *Phragmites australis* is a cosmopolitan species (Meyerson et al., 2016; Eller et al., 2017) but, across much of North America, an introduced lineage has aggressively spread into freshwater and brackish habitats (hereafter "invasive *P. australis*" or simply "*P. australis*"; Saltonstall, 2002; Meyerson et al., 2009). Consequences of its invasion include changes to community structure; a loss of local plant, fish, and bird biodiversity; and

altered nutrient and sedimentation dynamics (Chambers et al., 1999; Silliman and Bertness, 2004).

Invasive *P. australis* thrives in human-disturbed marshes. In particular, agricultural runoff, industrial expansion, shoreline development, and the removal of woody vegetation bordering marshes contribute to the reed's success by enriching porewater nutrients and removing native competitors (Chambers et al., 1999; Amsberry et al., 2000; Minchinton and Bertness, 2003; Silliman and Bertness, 2004). Invasive *P. australis* also has a strong photosynthetic response to elevated atmospheric CO_2 concentrations (eCO_2; Mozdzer and Megonigal, 2012). Moreover, its responses to eCO_2 and nitrogen enrichment (N_{enr}) are nearly additive; one study found that, individually, eCO_2 and N_{enr} stimulated its gross primary productivity (GPP) by 44% and 60%, respectively, but together they raised GPP by 95% (Caplan et al., 2015). Critically, *P. australis* also responds more strongly than native marsh species to CO_2 and N enrichment (Minchinton and Bertness, 2003; Mozdzer and Zieman, 2010; Mozdzer and Megonigal, 2012; Caplan et al., 2015). These unusually strong responses to resource addition have been attributed to high phenotypic plasticity in a number of physiological and morphological traits (Engloner, 2009; Mozdzer and Megonigal, 2012), including stomatal anatomy (Douhovnikoff et al., 2016).

Stomata play an integral role in mediating gas exchange so as to maximize carbon assimilation while regulating water loss (Razzaghi et al., 2011). Plants adjust leaf conductance to gases dynamically, by controlling stomatal aperture, and developmentally, by modifying stomatal morphology and density (Haworth et al., 2013, 2015). Fossil evidence (Franks et al., 2009), mathematical models (Konrad et al., 2008; de Boer et al., 2011), and growth chamber experiments (Woodward and Bazzaz, 1988) have shown that stomatal density generally declines in response to eCO_2, allowing plants across numerous taxa to maintain CO_2 assimilation rates while reducing transpiration. Nitrogen availability has also been linked to changes in stomatal aperture and plant water relations (Schulze et al., 1994; Maire et al., 2012; Lee et al., 2013; Song et al., 2019). Nitrogen limitation generally decreases stomatal conductance, leading to lower rates of photosynthesis and transpiration (Schulze et al., 1994; Lee et al., 2013). Conversely, nitrogen addition has been shown to improve water-use efficiency under drought through changes to stomatal regulation (Song et al., 2019).

In *P. australis*, high levels of phenotypic plasticity in stomatal features (Douhovnikoff et al., 2016; Spens and Douhovnikoff, 2016) may contribute to its physiological responses to eCO_2 and N_{enr}. For instance, under eCO_2, a decline in stomatal density may allow *P. australis* to reduce water loss while maintaining high photosynthestic rates (Franks and Farquhar, 2007; de Boer et al., 2011). Alterations to stomatal density and transpiration rates can also influence nutrient uptake through roots (Hepworth et al., 2015), while changes in stomatal size can influence the level of control plants have over stomatal aperture under varying hydrological conditions (in particular, plants can more rapidly adjust the aperture of smaller stomata; Franks and Farquhar, 2007; Franks et al., 2009). Despite the key role of stomata in mediating gas exchange, prior studies have not connected stomatal morphology of *P. australis* directly to its strong physiological response to eCO_2 and N_{enr}. For example, Mozdzer and Caplan (2018) reported eCO_2 and N_{enr} effects on stomatal characteristics and rates of photosynthesis but did not examine the relationship between them.

We estimated maximal conductance to water (g_{wmax}) of *P. australis* from measurements of stomatal characteristics in an open-top chamber experiment simulating near-future CO_2 concentrations and moderate levels of N enrichment. By pairing these measurements with those of gas exchange at the leaf level, we sought to mechanistically relate changes in stomatal features and photosynthetic physiology under global change conditions. We expected eCO_2 to stimulate photosynthesis but to induce reductions in stomatal density to reduce water loss. Further, since N limitation tends to decrease stomatal conductance (Schulze et al., 1994; Lee et al., 2013), we expected stomatal density to increase under N_{enr}. However, we predicted that stomatal length would decrease under N_{enr} given that changes in stomatal length tend to be opposite in direction to changes in density (Franks et al., 2009). We did not expect eCO_2 to alter stomatal length, as this has not been observed in other studies (e.g., Haworth et al., 2013), except for those encompassing evolutionary to geologic timescales (Franks et al., 2009). We expected eCO_2 and N_{enr} to have an additive effect on photosynthetic CO_2 assimilation, as previously demonstrated (e.g., Mozdzer and Caplan, 2018). Finally, under the assumption that changes to stomatal morphology underlie *P. australis*' growth responses to global change, we expected eCO_2 and N_{enr} to have similarly additive effects on relationships between stomatal characteristics, maximal stomatal conductance, and photosynthesis.

MATERIALS AND METHODS

Study site

The field component of this study was conducted at the Global Change Research Wetland (GCREW) in Edgewater, Maryland, United States (38.8742°N, 76.5474°W), which is administered by the Smithsonian Environmental Research Center. The GCREW is a brackish tidal marsh in the Rhode River subestuary of the Chesapeake Bay (mean = 10 practical salinity units [PSU], range = 3–15 PSU). Around 1970, *P. australis* became established and has since replaced much of the native high marsh community, which is otherwise dominated by *Schoenoplectus americanus*, *Spartina patens*, and *Distichlis spicata* (McCormick et al., 2010). Additional environmental data from the site are provided in Appendix S1.

Open-top chamber experiment

In 2011, 12 open-top chambers (1.25 × 2.5 × 4.4 m) were established along the leading edge of a *P. australis* stand at the GCREW. Every growing season since then, additions of eCO_2 and N_{enr} have been given to half of the chambers in a blocked factorial design. Within each of three blocks, chambers received either no addition, eCO_2, N_{enr}, or eCO_2+N_{enr}. The eCO_2 chambers were fumigated (+300 ppmv) from May through October. Nitrogen (+25 g N m^{-2} yr^{-1}) was applied monthly from May through September as ammonium chloride (5 g N m^{-2} $month^{-1}$). Enrichment levels simulate atmospheric CO_2 concentrations projected for 2100 under moderate CO_2 emissions models (Meinshausen et al., 2011) while N levels are characteristic of moderately nutrient-enriched estuaries on the Atlantic Coast of North America (Hopkinson and Giblin, 2008). Additional details of the enrichment experiment for *P. australis* at the GCREW were provided by Caplan et al. (2015).

Stomatal measurements

In July 2013 and 2018, we haphazardly selected three to five plants per experimental chamber and harvested the third or fourth most-apical, fully expanded leaf from each. Leaf discs were removed using a cork borer (14-mm diameter) and oven-dried to constant mass at 60°C. We then imaged stomata on the dried leaf discs using an environmental scanning electron microscope (TESCAN VEGA3, Brno, Czech Republic). Environmental scanning electron microscopy (ESEM) has several advantages over standard epidermal peel imaging, including greater resolution, higher magnification, and the ability to image dehydrated leaves with little chemical preparation (Khan et al., 2017). Because grasses are amphistomatous (Haworth et al., 2018), we imaged both adaxial and abaxial surfaces. Specifically, dried leaf samples were mounted on carbon tape stubs and imaged at two magnifications: 415× for measuring stomatal density (D; n = 356 measurements) and 2076× for stomatal length (L; n = 881 measurements). For each surface, we then calculated stomatal density (the number of stomata per unit area averaged across two 500 µm × 375 µm fields of view) and averaged the guard cell lengths of four to five haphazardly selected stomata per leaf.

Maximal stomatal conductance

Following Douhovnikoff et al. (2016), we estimated the maximum stomatal conductance to water vapor (g_{wmax}) using the equation given by Taylor et al. (2012) for grasses:

$$g_{\mathrm{wmax}} = \frac{d}{v} D \frac{a_{\max}}{l + (\frac{\pi}{2})\sqrt{a_{\max}/\pi}}, \quad (1)$$

where d is the diffusivity of water in air (2.49×10^{-5} m^2 s^{-1} at 25°C), v is the molar volume of air (0.0245 m^3 mol^{-1} at 25°C), D is stomatal density (measured directly), and π is the geometric constant (3.141). The calculation of g_{wmax} also requires stomatal pore area (a_{max}) and stomatal pore depth (l), which were derived from measured values of stomatal length (L; Taylor et al., 2012) as follows:

$$a_{max} = 0.4(0.25L^2) \quad (2)$$

$$l = 0.125\mathrm{L}. \quad (3)$$

Photosynthesis

Light-saturated photosynthetic rates (A_{sat}) were obtained by measuring light response curves in situ on the same leaves used for ESEM imaging but before harvest (n = 35 leaves in 2013 and 48 leaves in 2018). In July 2013 and 2018, we measured the relationship between photosynthetic rates and irradiance (i.e., we generated light response curves) using three LI-6400XT Photosynthesis Systems (LI-COR Biosciences, Lincoln, NE, USA). To do this, we exposed leaves to a sequence of nine light levels (2000, 1500, 1000, 700, 400, 200, 50, 25, 0 µmol photons m^{-2} s^{-1}) at growth CO_2 (400 ppmv for ambient and 700 ppmv for eCO_2). Additional details were described by Mozdzer and Caplan (2018). To obtain values of A_{sat}, we fit a nonrectangular hyperbolic function (Prioul and Chartier, 1977) to each data set using Prism v.8.4.3 (GraphPad Software, La Jolla, CA, USA).

Statistical analyses

We used linear mixed-effects models to compare the influence of CO_2, N, leaf surface, and their interactions (all fixed effects) on D, L, g_{wmax}, and A_{sat}. To account for experimental blocking and taking multiple measurements from chambers, all models included random effects for leaf identity, block, block × CO_2 level, and block × N level. Year was likewise included as a random effect because we were interested in accounting for the effects of interannual variation in environmental conditions (Appendix S1) rather than testing for them.

To examine the relationship between g_{wmax} and A_{sat}, we used the same mixed-effects modeling approach described above but A_{sat} was designated the response variable and g_{wmax} was included as a fixed effect; CO_2 level, N level, and their interactions were also included as fixed effects. We worked with chamber-level data for this analysis, with data from each year treated separately (n = 24). Given that different portions of leaves were often used for light-response curves and stomatal characterization, working with leaf-level data was untenable. Thus, models included many of the same random effects terms as above (year, block, block × CO_2 level, and block × N level), but we omitted the term for leaf identity.

We evaluated the influence of fixed effects on response variables using multi-model inference within the information-theoretic statistical framework (Grueber et al., 2011; Harrison et al., 2018). Specifically, we computed standardized, model-averaged coefficients (β) for each fixed effect, which depict the magnitude and direction of effect sizes and which can be compared across effects. We note that our goal was to compare effect sizes rather than to determine whether coefficients were distinguishable from zero (Burnham and Anderson, 2002). To compute β values, we standardized response variables and coded fixed effects (all of which were binary) as ±0.5 (Gelman, 2008; Grueber et al., 2011). We then fit each full model and its hierarchically complete subsidiary models using maximum-likelihood estimation. We quantified model fit based on the Akaike information criterion corrected for small sample sizes (AIC_c). Each β was then computed as the weighted average of all parameter estimates across models that had $\Delta AICc < 6$. When a model in the set did not contain a term, we used the conservative approach of taking its coefficient to be zero when averaging. The threshold for including models in the averaging process ($\Delta AICc < 6$) has been recommended by several authors for ecological studies (Richards, 2008; Harrison et al., 2018). Given that we selected models to compute model-averaged coefficients rather than to identify a single, best model, the choice of threshold would have had a minimal effect on our results. Model-averaged coefficients and associated statistics are presented in Table 1; only terms included in models with $\Delta AICc < 6$ appear.

In addition to using β values to assess effect sizes (with $|\beta| < 0.1$ deemed negligible), we used 95% confidence intervals (CIs) for the β values to assess the strength of evidence for their effects. Confidence intervals that excluded zero were taken as strong evidence for the effect being real and interpretable, with the width of the CI indicating how likely the effect was as strong as the β value indicated. Confidence intervals that extended slightly past zero were interpreted as providing modest evidence of an effect, and those extending well past zero were considered to provide weak evidence at best. R^2_{GLMM} values (Nakagawa and Schielzeth, 2013),

TABLE 1. Summary of statistical models for stomatal parameters and light-saturated photosynthesis. R^2_{GLMM} values are presented for full models. Coefficients are model-averaged.

Response	R^2_m	R^2_c	N_{obs}	N_{eval}	N_{mod}	Term	Coefficient	SE	95% CI
D	0.12	0.41	178	19	12	CO_2 level	0.074	0.097	(−0.115, 0.264)
						N level	0.183	0.111	(−0.036, 0.401)
						$CO_2 \times N$	−0.011	0.060	(−0.129, 0.106)
						Leaf surface	0.248	0.060	(0.131, 0.365)
L	0.08	0.38	178	19	13	CO_2 level	−0.105	0.097	(−0.295, 0.084)
						N level	0.124	0.103	(−0.078, 0.326)
						$CO_2 \times N$	−0.156	0.203	(−0.554, 0.242)
						Leaf surface	−0.001	0.033	(−0.067, 0.064)
g_{wmax}	0.13	0.44	178	19	12	CO_2 level	0.048	0.079	(−0.106, 0.203)
						N level	0.200	0.117	(−0.030, 0.430)
						$CO_2 \times N$	−0.023	0.080	(−0.180, 0.133)
						Leaf surface	0.241	0.058	(0.127, 0.354)
A_{sat}	0.29	0.83	83	5	3	CO_2 level	0.547	0.104	(0.343, 0.751)
						N level	0.074	0.118	(−0.156, 0.305)
						$CO_2 \times N$	−0.001	0.061	(−0.121, 0.118)

Notes: A_{sat}, light-saturated photosynthesis; g_{wmax}, estimated maximal stomatal conductance; *D*, stomatal density; *L*, stomatal length. R^2_m, fixed effects only (marginal); R^2_c, fixed + random effects (conditional); N_{obs}, number of observations after data cleaning; N_{eval}, total number of models evaluated; N_{mod}, number of models included in averaging (those with ΔAICc < 6).

calculated for each full model, were used to quantify how much of the variation in the response was explained by fixed and random effects. We assessed residual normality using quantile-quantile plots. All statistical analyses were performed using R 4.0.1 (R Foundation for Statistical Computing, Vienna, Austria). We used functions from the *lme4* and *MuMIn* libraries for mixed-effects modeling and multi-model inference, respectively. Figures were generated using Prism 8.4.3 (GraphPad Software).

RESULTS

The greatest difference between abaxial and adaxial leaf surfaces was in stomatal density (*D*). Mean *D* was 18% greater on adaxial than on abaxial surfaces (β = 0.248; Fig. 1A, Table 1; Appendix S2), which translated into maximal conductance (g_{wmax}) likewise being 18% greater on adaxial surfaces (β = 0.241). There were no identifiable differences in stomatal length (*L)* between leaf surfaces (β = −0.001; Fig. 1B), nor was there evidence that CO_2 or N addition had greater effects on one leaf surface versus the other (β < −0.02 for all interactions; Table 1). Therefore, the effects of eCO_2 and N_{enr} reported below are not separated by leaf surface.

Changes in *D* were primarily driven by N_{enr}, with mean *D* increasing by 20% under N addition (β = 0.183; Fig. 1A, Table 1; Appendix S3). The 95% CI for this effect extended slightly past zero (to −0.030), leaving open the possibility that there was no true effect. In contrast, the effect of eCO_2 on *D* (12% increase) was clearly weaker than that of N_{enr} (β = 0.074) and far less well-substantiated (Table 1). There was also no evidence of an interaction between N_{enr} and eCO_2 on *D* (β = −0.011).

Treatment effects on *L* were smaller than those on *D* (Fig. 1B); under N_{enr}, the sample mean for *L* increased by 4%, and there was only modest evidence of a minor effect (β = 0.124; Table 1; Appendix S3). Also, the effect of eCO_2 was negligible (0.44%; β = −0.105). Although the estimated size of the interaction effect was the largest of the three (β = −0.156; Table 1), the CI was too large to conclude that the effect was non-zero.

Treatment-induced changes in g_{wmax} were similar to those in *D* (Fig. 2A, Table 1; Appendix S3). Under N_{enr}, mean g_{wmax} increased by

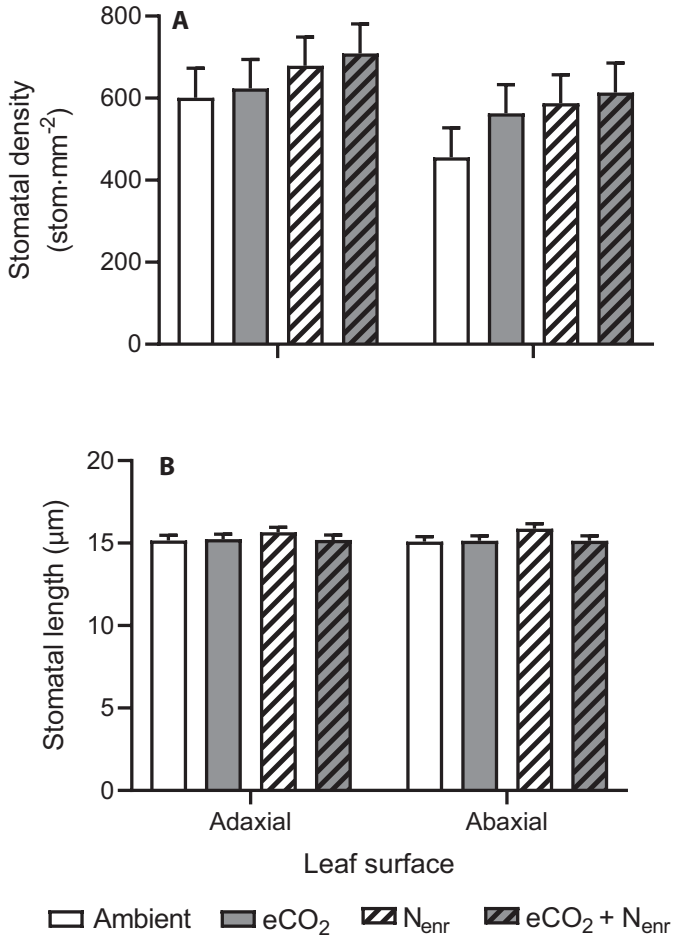

FIGURE 1. Influence of elevated CO_2 (eCO_2) and porewater N enrichment (N_{enr}) on *Phragmites australis* stomatal characteristics (marginal means ± SE) in an open-top growth chamber experiment in Maryland, USA. (A) Stomatal density, (B) stomatal length. See Table 1 and Appendix S3 for statistical results.

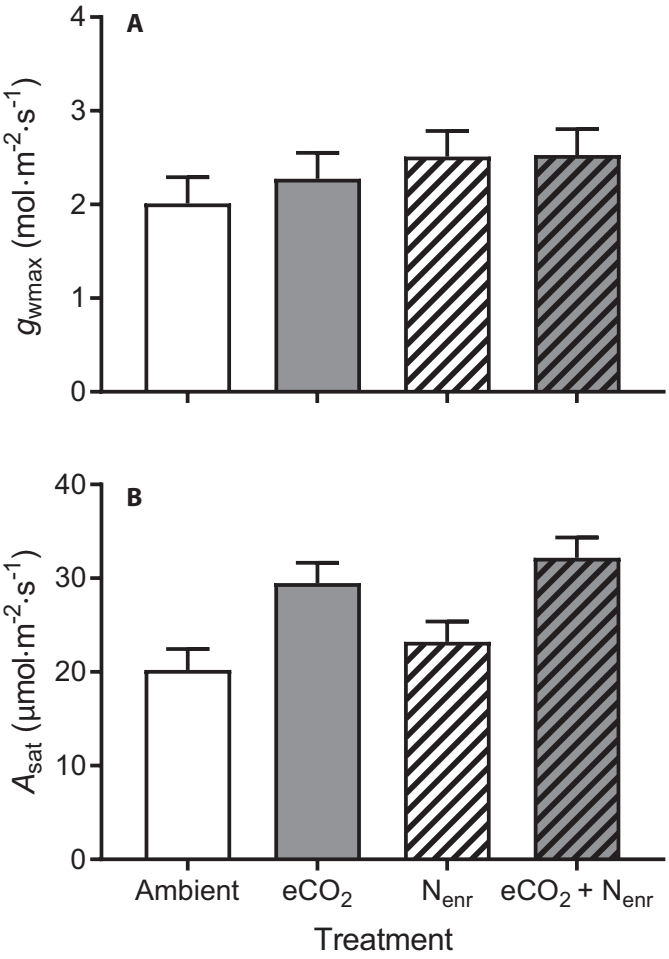

FIGURE 2. Stomatal and photosynthetic response (marginal means ± SE) of *Phragmites australis* to elevated CO_2 (eCO_2) and porewater N enrichment (N_{enr}). (A) Estimated maximal stomatal conductance (g_{wmax}), (B) rates of light-saturated photosynthesis (A_{sat}). Plants were grown in an open-top growth chamber experiment in Maryland, USA. g_{wmax} is averaged across adaxial and abaxial leaf surfaces. See Table 1 and Appendix S3 for statistical results.

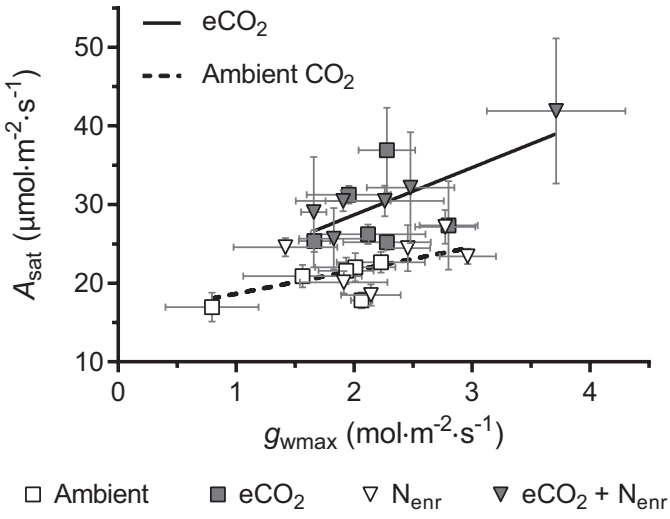

FIGURE 3. Relationship between estimated maximal stomatal conductance (g_{wmax}) and light-saturated photosynthesis rates (A_{sat}) of *Phragmites australis* in an open-top chamber experiment (Maryland, USA). g_{wmax} is averaged across adaxial and abaxial leaf surfaces. Points depict chamber-level marginal means (± SE) in two sampling years, separated by CO_2 level (ambient = white points and dashed line; eCO_2 = shaded points and solid line) and N level (ambient = squares; N_{enr} = triangles). See Appendix S4 for a statistical evaluation of this relationship.

25% with moderately strong evidence for the effect ($\beta = 0.200$; Table 1). However, under eCO_2, the data only provided weak evidence and the effect size was modest at best (13% increase; $\beta = 0.048$). The combined effect of the global change factors (N_{enr} + eCO_2) on g_{wmax} was similar to that of N_{enr} alone (26% increase; Appendix S3), with the standardized coefficient not indicative of the treatments interacting ($\beta = -0.023$; Table 1).

Light-saturated photosynthetic rates (A_{sat}) increased markedly (46%) in response to CO_2 enrichment ($\beta = 0.547$; Fig. 2B, Table 1; Appendix S3). There was insufficient evidence to conclude that N_{enr} stimulated A_{sat} ($\beta = 0.074$; Table 1), though the sample mean increased by 15%. In combination, eCO_2 + N_{enr} increased A_{sat} by 59%. Consistent with the additive nature of this response, there was little evidence of an $eCO_2 \times N_{enr}$ interaction on A_{sat} ($\beta = -0.001$; Table 1).

Both g_{wmax} and eCO_2 had moderate to strong effects on A_{sat} ($\beta = 0.344$ and 0.502, respectively; Fig. 3; Appendix S4). However, confidence intervals were wide, indicating that effects could have been larger or smaller than estimated. The data provided no evidence that eCO_2 or N_{enr} modified the slope of the relationship between g_{wmax} and A_{sat}, as interaction terms were not present in the set of models used for averaging (Appendix S4).

DISCUSSION

Elevated atmospheric CO_2 and nitrogen enrichment can enhance photosynthesis and biomass production, alleviate osmotic stress, and help coastal salt marshes keep pace with sea level rise (via organic matter and sediment accretion; McKee and Rooth, 2008; Cherry et al., 2009; Langley et al., 2009; Erickson et al., 2013). Because *P. australis* has far stronger responses to eCO_2 and N_{enr} than native marsh species in North America (Minchinton and Bertness, 2003; Rickey and Anderson, 2004; Silliman and Bertness, 2004; Caplan et al., 2015), these global change factors are accelerating its already widespread invasion and affording it considerable ecosystem-scale effects (Mozdzer and Megonigal, 2012; Eller et al., 2014; Mozdzer and Caplan, 2018). The present study helps to explain how invasive *P. australis* is able to achieve enhanced carbon gain in response to these two key global change factors. First, it shows that plastic shifts in stomatal features accompany increased photosynthetic rates in *P. australis* under eCO_2 and N_{enr}. Further, it demonstrates that light-saturated photosynthesis (A_{sat}) in *P. australis* is more strongly influenced by eCO_2, whereas maximal stomatal conductance (g_{wmax}) is more strongly influenced by N_{enr}.

Elevated CO_2 strongly stimulated A_{sat} (46%) but only modestly increased g_{wmax} (13%), if at all. This change in A_{sat} can be attributed to well-established processes: atmospheric CO_2 enrichment strengthens the CO_2 diffusion gradient across stomata, increasing CO_2 influx without requiring an increase in leaf conductance. In response, many plant species reduce stomatal density (and thus g_{wmax}) under eCO_2 to limit water loss while maintaining photosynthetic

rates (Franks and Farquhar, 2007; Franks et al., 2009). However, we found that invasive *P. australis* responded minimally to eCO_2 in either stomatal density (*D*) or length (*L*), suggesting that it increased its rates of carbon assimilation while maintaining similar rates of water loss. It was not clear from our results whether *P. australis* experienced an increase in water-use efficiency under eCO_2; the lack of an eCO_2 interaction effect with g_{wmax} in the A_{sat} model likewise provides little insight. A possible explanation for the lack of a shift in stomatal density under eCO_2 (i.e., foregoing the opportunity to reduce water loss) is that *P. australis* possesses complementary physiological adaptations that allow it to maintain adequate stomatal conductance even when faced with salinity-induced water stress (Eller et al., 2017 and references within).

The responses of *P. australis* to N_{enr} were primarily morphological rather than physiological (i.e., there were shifts in stomatal characteristics rather than A_{sat}). N_{enr} induced *P. australis* to increase stomatal density (+20%), which also appeared to translate into increases in g_{wmax} (+25%). While g_{wmax} is influenced by both stomatal length and density (Taylor et al., 2012), our results suggested that this N_{enr} effect on g_{wmax} was mainly driven by changes in stomatal density (+20%), whereas N_{enr} had little to no effect on length (+4%). Moreover, maximal conductance, g_{wmax}, is known to constrain operational stomatal conductance, g_{op} (Drake et al., 2013), so this N_{enr}-induced increase in g_{wmax} could be expected to enhance the carbon-intake capacity of *P. australis* under N_{enr}, especially given the positive relationship between g_{wmax} and A_{sat}. Surprisingly, however, we found no evidence that N_{enr} influenced A_{sat}, contrary to the results of a previous study from the same site (Mozdzer and Caplan, 2018) that documented a modest increase in A_{sat} under N_{enr} conditions (+17%). A possibility raised by Mozdzer and Caplan (2018) is that salinity may diminish N_{enr}-induced A_{sat} stimulation. However, it is unclear from the available data whether porewater salinity was particularly high during our measurement periods (July 2013 and 2018) since we did not measure salinity at the experimental *P. australis* stand. Still, our results are consistent with Mozdzer and Caplan's (2018) finding that N_{enr} primarily induces morphological changes in *P. australis*.

We documented shifts in stomatal characteristics under eCO_2 and N_{enr} that apparently afforded invasive *P. australis* substantially greater rates of photosynthesis. eCO_2 more strongly influenced photosynthesis (primarily by strengthening the CO_2 concentration gradient), while N_{enr} more strongly influenced maximal stomatal conductance (primarily by increasing stomatal density). These adjustments in leaf structure and function appear to be key mechanisms underlying complementary morphological and physiological responses of *P. australis* to important limiting resources, helping to explain its invasion in N-enriched marshes and portending what it may be capable of in an elevated CO_2 world.

ACKNOWLEDGMENTS

We thank Rachel Beane and Celeste Morin for training on and permission to use the ESEM. We also thank J. Patrick Megonigal and Patrick Neale for providing meteorological data, which were compiled by Rutuja Chitra-Tarak. We are grateful to Samuel Taylor for clarifying the physical constants used in the g_{wmax} calculations and to Brittany Jellison and Sarah Kingston for assistance with R. We thank Bruce Kohorn and two anonymous reviewers for insights and feedback on early drafts. This work was supported by a Freedman Summer Research Fellowship in Coastal/Environmental Studies to J.R.G., the National Science Foundation (MRI 1530963, DEB LTREB-1557009, and DEB DEB 2051343) and Bryn Mawr College.

AUTHOR CONTRIBUTIONS

B.A.L., J.R.G., T.J.M., and V.D. designed the study. J.R.G. performed ESEM image analysis and led the creation of the manuscript, on which all authors offered input. T.J.M. led gas exchange measurements and leads the experiment at GCREW. J.R.G. and J.S.C. led data analyses.

DATA AVAILABILITY

All *P. australis* and environmental data are available at FigShare along with Appendices S1–4 (https://doi.org/10.6084/m9.figshare.c.5232344). Meteorological data from the SERC weather tower from the SERC website (https://serc.si.edu/gcrew/phragmites data) and buoy data for Annapolis, MD from the Chesapeake Bay Interactive Buoy System website (https://buoybay.noaa.gov/observations/data-download) were downloaded on 4 April 2019.

SUPPORTING INFORMATION

Additional Supporting Information may be found online in the supporting information tab for this article.

APPENDIX S1. Environmental data from the SERC weather tower and a nearby observational buoy in the Chesapeake Bay.

APPENDIX S2. Estimated marginal means (±SE) of stomatal characteristics in *Phragmites australis* for adaxial vs abaxial leaf surface.

APPENDIX S3. Estimated marginal means (±SE) of gas exchange and maximal stomatal conductance in *Phragmites australis*.

APPENDIX S4. Summary of model averaged mixed-effects models examining relationship between g_{wmax} and A_{sat} in *Phragmites australis*.

LITERATURE CITED

Amsberry, L., M. A. Baker, P. J. Ewanchuk, and M. D. Bertness. 2000. Clonal integration and the expansion of *Phragmites australis*. *Ecological Applications* 10: 1110–1118.

Burnham, K. P., and D. R. Anderson. 2002. Model selection and multimodel inference: a practical information-theoretic approach. Springer, NY, NY, USA.

Caplan, J. S., R. N. Hager, J. P. Megonigal, and T. J. Mozdzer. 2015. Global change accelerates carbon assimilation by a wetland ecosystem engineer. *Environmental Research Letters* 10: 1–12.

Cesarino, I., I. R. Dello, G. K. Kirschner, M. S. Ogden, K. L. Picard, M. I. Rast-Somssich, and M. Somssich. 2020. Plant science's next top models. *Annals of Botany* 126: 1–23.

Chambers, R. M., L. A. Meyerson, and K. Saltonstall. 1999. Expansion of *Phragmites australis* into tidal wetlands of North America. *Aquatic Botany* 64: 261–273.

Cherry, J. A., K. L. McKee, and J. B. Grace. 2009. Elevated CO_2 enhances biological contributions to elevation change in coastal wetlands by offsetting stressors associated with sea-level rise. *Journal of Ecology* 97: 67–77.

de Boer, H. J., E. I. Lammertsma, F. Wagner-Cremer, D. L. Dilcher, M. J. Wassen, and S. C. Dekker. 2011. Climate forcing due to optimization of maximal leaf conductance in subtropical vegetation under rising CO_2. *Proceedings of the National Academy of Sciences, USA* 108: 4041–4046.

Douhovnikoff, V., S. H. Taylor, E. L. G. Hazelton, C. M. Smith, and J. O'Brien. 2016. Maximal stomatal conductance to water and plasticity in stomatal traits differ between native and invasive introduced lineages of *Phragmites australis* in North America. *AoB Plants* 8: 1–8.

Drake, P. L., R. H. Froend, and P. J. Franks. 2013. Smaller, faster stomata: scaling of stomatal size, rate of response, and stomatal conductance. *Journal of Experimental Botany* 64: 495–505.

Eller, F., C. Lambertini, L. X. Nguyen, and H. Brix. 2014. Increased invasive potential of non-native *Phragmites australis*: elevated CO_2 and temperature alleviate salinity effects on photosynthesis and growth. *Global Change Biology* 20: 531–543.

Eller, F., H. Skálová, J. S. Caplan, G. P. Bhattarai, M. K. Burger, J. T. Cronin, W.-Y. Guo, et al. 2017. Cosmopolitan species as models for ecophysiological responses to global change: the common reed *Phragmites australis*. *Frontiers in Plant Science* 8: 1833.

Engloner, A. I. 2009. Structure, growth dynamics and biomass of reed (*Phragmites australis*) – a review. *Flora* 204: 331–346.

Erickson, J. E., G. Peresta, K. J. Montovan, and B. G. Drake. 2013. Direct and indirect effects of elevated atmospheric CO_2 on net ecosystem production in a Chesapeake Bay tidal wetland. *Global Change Biology* 19: 3368–3378.

Franks, P. J., D. J. Beerling, and R. A. Berner. 2009. Maximum leaf conductance driven by CO_2 effects on stomatal size and density over geologic time. *Proceedings of the National Academy of Sciences, USA* 106: 10343–10347.

Franks, P. J., and G. D. Farquhar. 2007. The mechanical diversity of stomata and its significance in gas-exchange control. *Plant Physiology* 143: 78–87.

Gelman, A. 2008. Scaling regression inputs by dividing by two standard deviations. *Statistics in Medicine* 27: 2865–2873.

Groom, M. J. 2006. Threats to biodiversity. *Principles of Conservation Biology* 3: 63–109.

Grueber, C. E., S. Nakagawa, R. J. Laws, and I. G. Jamieson. 2011. Multimodel inference in ecology and evolution: challenges and solutions. *Journal of Evolutionary Biology* 24: 699–711.

Harrison, X. A., L. Donaldson, M. E. Correa-Cano, J. Evans, D. N. Fisher, C. E. D. Goodwin, B. S. Robinson, D. J. Hodgson, and R. Inger. 2018. A brief introduction to mixed effects modelling and multi-model inference in ecology. *PeerJ* 6: e4794.

Haworth, M., C. Elliott-Kingston, and J. C. McElwain. 2013. Co-ordination of physiological and morphological responses of stomata to elevated [CO_2] in vascular plants. *Oecologia* 171: 71–82.

Haworth, M., D. Killi, A. Materassi, and A. Raschi. 2015. Coordination of stomatal physiological behavior and morphology with carbon dioxide determines stomatal control. *American Journal of Botany* 102: 677–688.

Haworth, M., C. P. Scutt, C. Douthec, G. Marinoa, M. T. G. Gomesa, F. Loretoe, J. Flexasc, et al. 2018. Allocation of the epidermis to stomata relates to stomatal physiological control: stomatal factors involved in the evolutionary diversification of the angiosperms and development of amphistomaty. *Environmental and Experimental Botany* 151: 55–63.

Hepworth, C., T. Doheny-Adams, L. Hunt, D. D. Cameron, and J. E. Gray. 2015. Manipulating stomatal density enhances drought tolerance without deleterious effect on nutrient uptake. *New Phytologist* 208: 336–341.

Hopkinson, C., and A. E. Giblin. 2008. Nitrogen dynamics of coastal salt marshes. *In* D. G. Capone, D. A. Bronk, M. R. Mulholland, and E. J. Carpenter [eds.], Nitrogen in the marine environment, 2nd edn, 991–1036. Academic Press, Cambridge, MA, USA.

Katsanevakis, S., I. Wallentinus, A. Zenetos, E. Leppakoski, M. E. Cinar, B. Ozturk, M. Grabowski et al. 2014. Impacts of invasive alien marine species on ecosystem services and biodiversity: a pan-European review. *Aquatic Invasions* 9: 391–423.

Khan, R., M. Ahmad, M. Zafar, and A. Ullad. 2017. Scanning electron and light microscopy of foliar epidermal characters: a tool for plant taxonomists in the identification of grasses. *Microscopy, Research, & Technique* 80: 1123–1140.

Konrad, W., A. Roth-Nebelsick, and M. Grein. 2008. Modelling of stomatal density response to atmospheric CO_2. *Journal of Theoretical Biology* 253: 638–658.

Langley, J. A., K. L. McKee, D. R. Cahoon, J. A. Cherry, and P. J. Megonigal. 2009. Elevated CO_2 stimulates marsh elevation gain, counterbalancing sea-level rise. *Proceedings of the National Academy of Sciences, USA* 106: 6182–6186.

Lee, E., B. S. Felzer, and Z. Kothavala. 2013. Effects of nitrogen limitation on hydrological processes in CLM4-CN. *Journal of Advances in Modeling Earth Systems* 5: 741–754.

Maire, V., P. Martre, J. Kattge, F. Gastal, G. Esser, S. Fontaine, and J.-F. Soussana. 2012. The coordination of leaf photosynthesis links C and N fluxes in C_3 plant species. *PLoS One* 7: e38345.

McCormick, M. K., K. M. Kettenring, H. M. Baron, and D. F. Whigham. 2010. Extent and reproductive mechanisms of *Phragmites australis* spread in brackish wetlands in Chesapeake Bay, Maryland (USA). *Wetlands* 30: 67–74.

McKee, K. L., and J. E. Rooth. 2008. Where temperate meets tropical: multifactorial effects of elevated CO_2, nitrogen enrichment, and competition on a mangrove–salt marsh community. *Global Change Biology* 14: 971–984.

Meinshausen, M., S. J. Smith, K. Calvin, J. S. Daniel, M. L. T. Kainuma, J.-F. Lamarque, K. Matsumoto, et al. 2011. The RCP greenhouse gas concentrations and their extensions from 1765 to 2300. *Climatic Change* 109: 213–241.

Meyerson, L. A., J. T. Cronin, and P. Pyšek. 2016. *Phragmites australis* as a model organism for studying plant invasions. *Biological Invasions* 18: 2421–2431.

Meyerson, L. A., K. Saltonstall, and R. M. Chambers. 2009. *Phragmites australis* in eastern North America: a historical and ecological perspective. *In* B. R. Silliman, E. Grosholz, and M. D. Bertness [eds.], Human impacts on salt marshes: a global perspective, 57–82. University of California Press, Los Angeles, CA, USA.

Minchinton, T. E., and M. D. Bertness. 2003. Disturbance-mediated competition and the spread of *Phragmites australis* in a coastal marsh. *Ecological Applications* 13: 1400–1416.

Mozdzer, T. J., and J. S. Caplan. 2018. Complementary responses of morphology and physiology enhance the stand-scale production of a model invasive species under elevated CO_2 and nitrogen. *Functional Ecology* 32: 1784–1796.

Mozdzer, T. J., and J. P. Megonigal. 2012. Jack-and-master trait responses to elevated CO_2 and N: a comparison of native and introduced *Phragmites australis*. *PLoS One* 7: e42794.

Mozdzer, T. J., and J. C. Zieman. 2010. Ecophysiological differences between genetic lineages facilitate the invasion of non-native *Phragmites australis* in North American Atlantic coast wetlands. *Journal of Ecology* 98: 451–458.

Nakagawa, S., and H. Schielzeth. 2013. A general and simple method for obtaining R^2 from generalized linear mixed-effects models. *Methods in Ecology and Evolution* 4: 133–142.

Prioul, J. L., and P. Chartier. 1977. Partitioning of transfer and carboxylation components of intracellular resistance to photosynthetic CO_2; fixation: a critical analysis of the methods used. *Annals of Botany* 41: 789–800.

Razzaghi, F., S. H. Ahmadi, V. I. Adolf, C. R. Jensen, S.-E. Jacobsen, and M. N. Andersen. 2011. Water relations and transpiration of quinoa (*Chenopodium quinoa* Willd.) under salinity and soil drying. *Journal of Agronomy and Crop Science* 197: 348–360.

Rickey, M. A., and R. C. Anderson. 2004. Effects of nitrogen addition on the invasive grass *Phragmites australis* and a native competitor *Spartina pectinata*. *Journal of Applied Ecology* 41: 888–896.

Richards, S. A. 2008. Dealing with overdispersed count data in applied ecology. *Journal of Applied Ecology* 45: 218–227.

Saltonstall, K. 2002. Cryptic invasion by a non-native genotype of the common reed, *Phragmites australis*, into North America. *Proceedings of the National Academy of Sciences, USA* 99: 2445–2449.

Schulze, E., F. Kelliher, C. Körner, J. Lloyd, and R. Leuning. 1994. Relationships among maximum stomatal conductance, ecosystem surface conductance, carbon assimilation rate, and plant nitrogen nutrition: a global ecology scaling exercise. *Annual Review of Ecology and Systematics* 25: 629–662.

Silliman, B. R., and M. D. Bertness. 2004. Shoreline development drives invasion of *Phragmites australis* and the loss of plant diversity on New England salt marshes. *Conservation Biology* 18: 1424–1434.

Song, J., Y. Wang, Y. Pan, J. Pang, X. Zhang, J. Fan, and Y. Zhang. 2019. The influence of nitrogen availability on anatomical and physiological responses of *Populus alba* × *P. glandulosa* to drought stress. *BMC Plant Biology* 19: 63.

Spens, A. E., and V. Douhovnikoff. 2016. Epigenetic variation within *Phragmites australis* among lineages, genotypes, and ramets. *Biological Invasions* 18: 2457–2462.

Taylor, S. H., P. J. Franks, S. P. Hulme, E. Spriggs, P. A. Christin, E. J. Edwards, F. I. Woodward et al. 2012. Photosynthetic pathway and ecological adaptation explain stomatal trait diversity amongst grasses. *New Phytologist* 193: 387–396.

Vila, M., and P. E. Hulme. 2017. Non-native species, ecosystem services, and human well-being. *In* M. Vila and P. E. Hulme [eds.], Impacts of biological invasions on ecosystem services, 1–14.Springer, Cham, Switzerland.

Woodward, F. I., and F. A. Bazzaz. 1988. The responses of stomatal density to CO_2 partial pressure. *Journal of Experimental Botany* 39: 1771–1781.